TI Designs: TIDA-01588
ブラシ付き*DC*サーボ・ドライブ用、*10.8V/15W*、*効率90%超*、*2.4cm²*電力段のリファレンス・デザイン

TEXAS INSTRUMENTS

概要

この15W、12mm×20mm電力段のリファレンス・デザインは、3〜6セル・リチウムイオン・バッテリで動作するブラシ付きDC (BDC)モータを駆動し、その位置を制御します。この高効率ソリューションは、超小型のフォーム・ファクタに最適化されているためモータに収まりやすく、高精度のモータ位置制御をサポートします。また、位置フィードバックなしで、モータを高速駆動することもできます。高速かつ高精度の電流センシングにより高品質のトルク制御を実現する一方、オンボードMCUにUART接続機能が搭載されているため、外付けコントローラによる制御も可能です。

リソース

|	
TIDA-01588	デザイン・フォルダ
DRV8870	プロダクト・フォルダ
MSP430FR2433	プロダクト・フォルダ
TLV9061	プロダクト・フォルダ
TPS709	プロダクト・フォルダ
TVS3300	プロダクト・フォルダ
ESD122	プロダクト・フォルダ

TI E2E™ Community

E2E™エキスパートに質問

特長

- ブラシ付きDCサーボ・ドライブは6.5V〜25.2Vの電圧範囲(3〜6セル・リチウムイオン・バッテリ)で動作
- 連続1.4A RMS、ピーク2.75Aのモータ巻線電流に対応
- エンコーダまたはポテンショメータによる位置フィードバックで高精度のモータ位置制御を実現
- 12mm×20mmの超小型PCBフォーム・ファクタ
- 較正精度誤差1%未満の電流センシングにより、正確なモータ・トルク制御を実現
- ヒート・シンクなしで、90%を超える電力段効率
- 過電流、貫通電流、低電圧、および過熱保護
- UART有線通信をサポート
- 動作時周囲温度: −20℃〜55℃
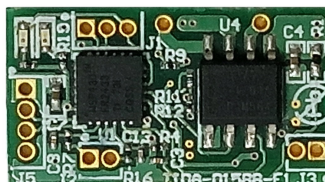- 高度に統合された高効率のモータ・ドライバを使用することで、全体的なBOMの削減、PCBフォーム・ファクタの小型化、冷却機能の削減が可能になります。

アプリケーション

- ヒューマノイド(ヒト型ロボット)
- ロボット型掃除機
- ロボット芝刈り機
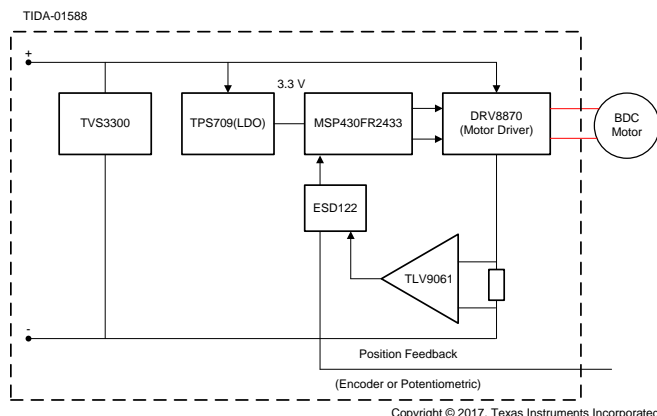
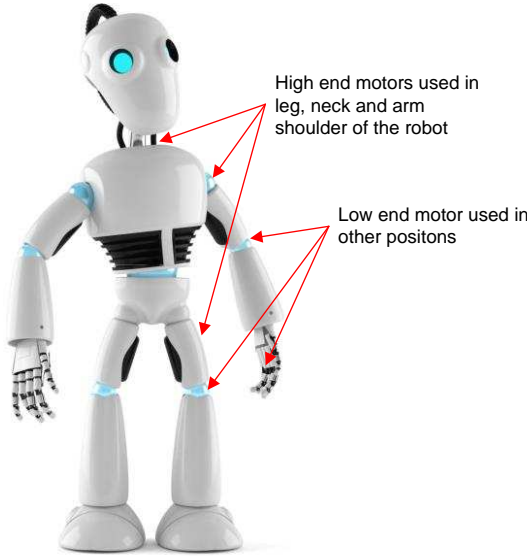Copyright © 2017, Texas Instruments Incorporated

1 System Description

A humanoid robot is a type of service robot used in wide-end applications, such as research applications where human access is risky, high-end toys used for teaching, dancing, and speaking, and more. Multiple motors are present in a typical humanoid depending upon the features and application requirement. The commonly used motors are BDC, brushless DC (BLDC), and sometimes stepper types. 図 1 shows the examples of motor drive locations in a typical humanoid. The high-end or high-power motors are typically present in the neck, legs, shoulders, and so on. Low-end or low-power motors are used in other locations such as elbows, knees, fingers, and so on Low-end motors normally use BDC motors with power levels less than 15 W. The electronic drive used in these motors has the following requirements:

- Must be small enough to fit with the motor
- Must support accurate position and torque control
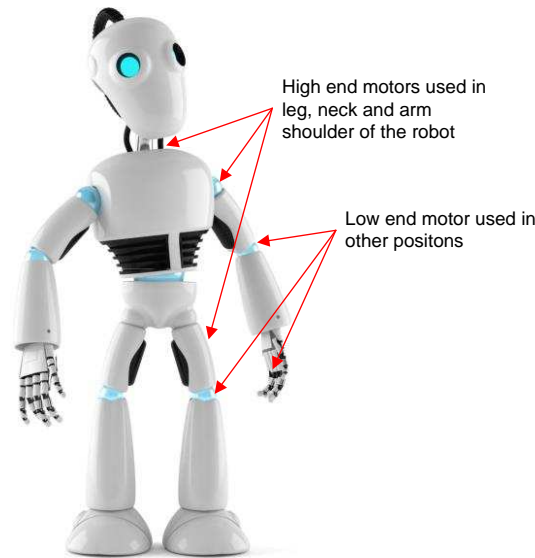- Must have the sufficient holding torque capability

High end motors used in leg, neck and arm shoulder of the robot

Low end motor used in other positons

図 1. Typical Humanoid—Motor Drive Locations

Vacuum robots are another service robot widely used in consumer applications for cleaning. The motors used in vacuum robots have different requirements like high-speed rotation, high torque-slow speed operation, or position control depending on the functionality these motors support (for example, suction, wheel, side brush, position control of the robotic vision control motor, and so on). BDC, BLDC, or stepper motors are typically used. The electronic drives have similar requirements as said in the case of humanoids.

This reference design can support the position control in a humanoid or the motor control in a vacuum robot. The design demonstrates the BDC motor servo drive power stage in a very small form factor using the highly-integrated motor driver DRV8870 featuring a low $R_{DS(ON)}$ of 565 mΩ (HS+LS), in a 4.9-mm × 6-mm package. The device features integrated current regulation and protection features, which enables the reduction of overall BOM. The thermal PowerPAD™ integrated circuit package eases the heat dissipation to the PCB. The TPS709 LDO features a low-quiescent current (<1 μA) and generates the low-noise, stable, 3.3-V power supply for the MCU. The TLV9061 amplifier enables accurate current sensing for precise torque control, and the small package allows over all PCB form factor reduction. The MSP430FR2433 runs the position control algorithm by taking the position feedback signals from the motor. The ESD122 and the TVS3300 provide ESD and surge voltage protection on different voltage lines.

The test report evaluates the board power capability, efficiency, current sensing accuracy, overcurrent protection, peak current capability, and the position control with sufficient hold up torque.

1.1 *Key System Specifications*

表 1. Key System Specifications

PARAMETERS	SPECIFICATIONS
Input voltage	10.8-V DC (6.5-V minimum to 25.2-V maximum)
Rated output power	15 W
RMS winding current	1.4 A
Peak winding current	2 A (for 2 s), 2.75 A (for 1 s)
Power stage switching frequency	20 kHz (adjustable)
Feedback signals	DC bus voltage, encoder or potentiometric position feedback, low-side DC bus current
Protections	Overcurrent, input undervoltage, overtemperature, shoot-through
Cooling	Natural cooling only, no heat sink
Operating ambient	−20°C to 55°C
Board specification	12-mm x 20-mm, 2-layer, 1-oz copper, 1.6-mm board thickness
Efficiency	> 90%

2   System Overview

2.1   *Block Diagram*

TIDA-01588

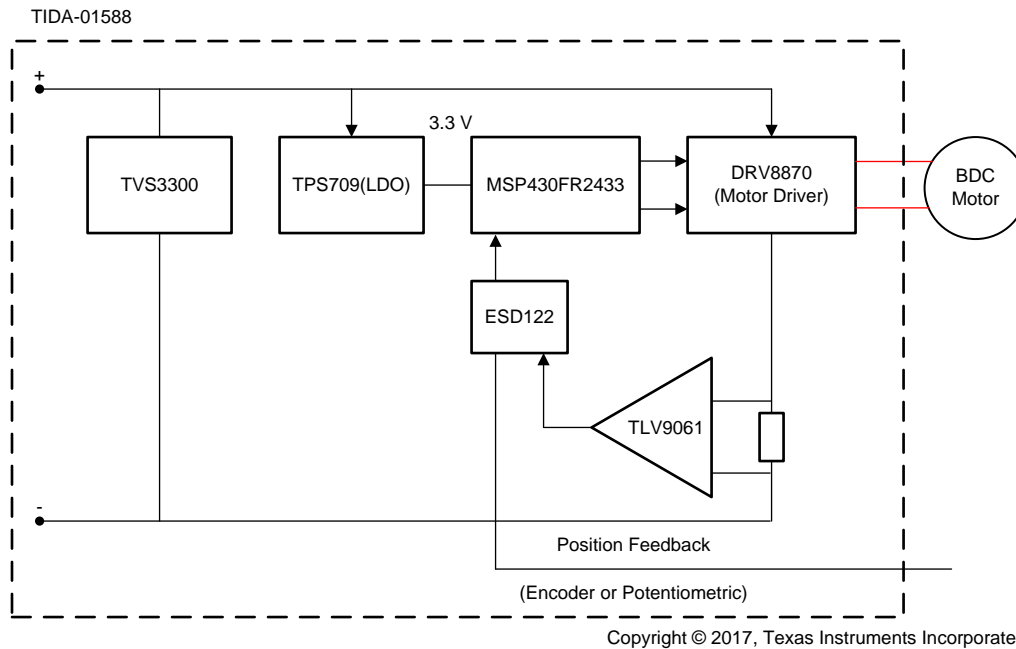Copyright © 2017, Texas Instruments Incorporated

図 2. TIDA-01588 Block Diagram

2.2   *Highlighted Products*

2.2.1   DRV8870

The key requirements in selecting the motor driver are:

• Small chip size BDC motor driver (full bridge) with high level of integration and protection

• Support 1.5-A RMS continuous and 3-A peak

• Minimal power loss and good heat dissipation

The reference design uses the highly-integrated BDC motor driver DRV8870. Two logic inputs control the H-bridge driver, which consists of four N-channel MOSFETs that can control motors bidirectionally with up to 3.6-A peak current. The inputs can be pulse-width modulated (PWM) to control motor speed using a choice of current-decay modes. Setting both inputs low enters the driver into a low-power sleep mode.

The DRV8870 device features integrated current regulation based on the analog input VREF and the voltage on the ISEN pin, which is proportional to motor current through an external sense resistor. The ability to limit current to a known level can significantly reduces the system power requirements and bulk capacitance required to maintain stable voltage especially for motor startup and stall conditions. The device is fully protected from faults and short circuits including undervoltage (UVLO), overcurrent (OCP), and overtemperature (TSD). When the fault condition is removed, the device automatically resumes normal operation.

2.2.2 MSP430FR2433

The MSP430FR2433 microcontroller (MCU) is part of the MSP430™ MCU value line sensing portfolio, TI's lowest-cost family of MCUs. The architecture, FRAM, and integrated peripherals, combined with extensive low-power modes, are optimized to achieve extended battery life in portable and battery-powered applications in a small VQFN package (4 mm × 4 mm). FRAM technology combines the low-energy fast writes, flexibility, and endurance of RAM with the non-volatility of flash.

The MSP430FR2433 has MCU configurations with two 16-bit timers, two universal serial communication interfaces (USCIs), a 32-bit hardware multiplier and a high-performance 10-bit 200-ksps analog-to-digital converter (ADC). The device is capable of working up to a clock frequency of 16 MHz. The ports 1 and 2 of the MSP430FR2433 have interrupt capabilities.

The availability of required peripherals in a small package along with the low-power consumption makes the device ideal for a battery-powered motor drive application in service robots.

2.2.3 TLV9061

The TLV9061 (single), TLV9062 (dual), and TLV9064 (quad) are single-, dual-, and quad- low-voltage (1.8 V to 5.5 V) operational amplifiers (op amps) with rail-to-rail input- and output-swing capabilities. These devices are highly cost-effective solutions for applications where low-voltage operation, small footprint, and high-capacitive load drive are required. Although the capacitive load drive of the TLV9061 is 100 pF, the resistive open-loop output impedance makes stabilizing with higher-capacitive loads simpler. The TLV9061 has a single rail supply, low quiescent current (568 μA), unity gain bandwidth of 10 MHz. The TLV906x family helps to simplify system design because the family is unity-gain stable, integrates the RFI and EMI rejection filter, and provides no phase reversal in overdrive condition.

Micro-size packages, available down to 0.8 mm × 0.8 mm, help the designer to achieve very small form factor.

2.2.4 TPS709

The TPS70933 linear regulator is an ultra-low quiescent current device designed for power-sensitive applications. The LDO can work up to a 30-V input voltage, which makes it ideal for up to six-cell Li-ion battery supply application. A precision band-gap and error amplifier provides 2% accuracy over temperature. A quiescent current of only 1 μA makes this LDO ideal for battery-powered, always-on systems that require very little idle-state power dissipation. This device has thermal-shutdown, current limit, and reverse-current protections for added safety. The TPS70933 linear regulator is available in WSON-6 and SOT-23-5 packages.

2.2.5 TVS3300

The TVS3300 is a transient voltage suppressor that provides robust protection for electronic circuits exposed to high-transient voltage events. Unlike a traditional TVS diode, the TVS3300 precision clamp triggers at a lower breakdown voltage and regulates to maintain a flat clamping voltage throughout a transient overvoltage event. The lower clamping voltage combined with a low dynamic resistance enables a unique TVS protection solution that can lower the voltage a system is exposed during a surge event by up to 30% in unidirectional configuration and up to 20% in bidirectional configuration when compared to traditional TVS diodes.

The TVS3300 is a unidirectional precision surge protection clamp with a 33-V working voltage designed specifically to protect systems with mid-voltage rails in industrial, communication, and factory automation applications. The TVS3300 has a fast response time when surge current is applied, so there is no overshoot voltage during clamping, which makes the device ideal to replace traditional TVS and zener diodes.

The TVS3300 is available in two small footprint packages that can reduce footprint by 94% (WCSP package) and 79% (SON package) for space-constrained applications when used in place of an industry standard SMB package. Both package options robustly dissipate the surge power and provide up to 58% lower leakage current compared to traditional TVS diodes in SMA and SMB package.

2.2.6   ESD122

The ESD122 is a bidirectional TVS ESD protection diode array. The ESD122 is rated to dissipate contact ESD strikes at the maximum level specified in the IEC 61000-4-2 international standard (17-kV contact, 17-kV air-gap). This device features a low I/O capacitance per channel. The low-dynamic resistance and low-clamping voltage ensure system level protection against transient events.

2.3   System Design Theory

2.3.1   DC Voltage Input to Board

The board gets the DC input voltage through the jumper J3. The TVS3300 is a surge protection clamp provided at the input to protect the circuit from input voltage surges. The design is optimized for a three-cell Li-ion battery and can support up to six-cell applications with a maximum voltage of 25.2 V.
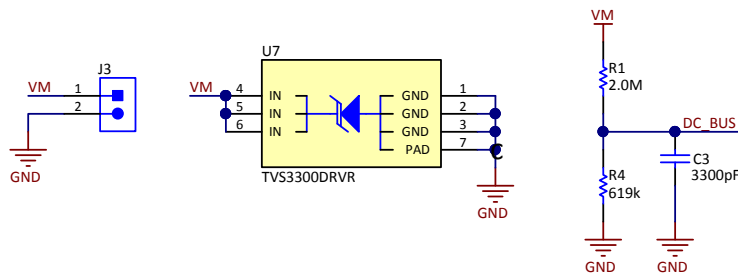
Copyright © 2017, Texas Instruments Incorporated

図 3. Schematic of Battery Power Input Section

The input supply voltage VM is scaled using the resistive divider network, which consists of R1, R4, and C3, and is fed to the MCU. Considering the maximum voltage for the MCU, ADC input is 3.3 V, and the maximum DC input voltage measurable by the MCU is calculated as 式 1.

$$V\frac{max}{DC} = V\frac{max}{ADC\_DC} \times \frac{(619\text{ k}\Omega + 2000\text{ k}\Omega)}{619\text{ k}\Omega} = 3.3 \times \frac{(619\text{ k}\Omega + 2000\text{ k}\Omega)}{619\text{ k}\Omega} = 13.96\text{ V}$$

(1)

Considering a 10% headroom for this value, the maximum recommended voltage input to the system is 13.96 × 0.9 = 12.56 V. For a power stage operating from three-cell Li-ion with a maximum operating voltage of 12.6 V, this voltage feedback resistor divider is ideal. Also, this choice gives optimal ADC resolution for a system operating from 6 V to 12.6 V.

> 注: Adjust the value of R4 for supporting the voltage sensing up to 25.2-V input voltage. For example select R4 = 309 k to support up to 25.2 V.

2.3.2 DRV8870—BDC Motor Driver

図 4 shows the schematic of the DRV8870 motor driver. The DRV8870 device is made of four N-channel MOSFETs that can control motors bidirectionally with up to 3.6-A peak current.
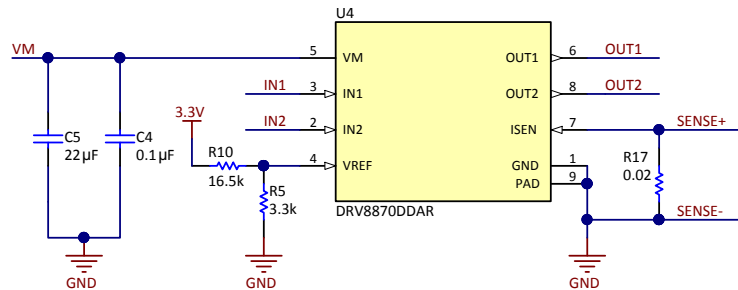
Copyright © 2017, Texas Instruments Incorporated

図 4. Schematic of DRV8870-BDC Motor Driver

A 22-μF capacitor (C5) is used as the VM input bulk capacitor. Another 0.1-μF bypass capacitor (C4) is also provided. C5 and C4 are selected to support up to 25.2 V. IN1 and IN2 are the PWM inputs from the MCU, which control the half-bridge MOSFETs. OUT1 and OUT2 are the phase node of the H-bridge, which must be connected to the external BDC motor winding.

The sense resistor (R17) is chosen appropriately for sensing the H-bridge low-side current. The sense resistor R17 along with voltage at the VREF pin of DRV8870 decides the internal peak current limit of DRV8870. The voltage across R17 is also fed to the current sense amplifier circuit (described in 2.3.4) to monitor the motor current precisely.

The DRV8870 device limits the output current based on the analog voltage input at VREF, and the external sense resistor R17 on the ISEN pin according to 式 2.

$$I_{TRIP}(A) = \frac{VREF\,(V)}{A_V \times R_{ISEN\,(\Omega)}} = \frac{VREF\,(V)}{10 \times R_{ISEN\,(\Omega)}}$$

(2)

Resistors R10 (16.5 kΩ) and R5 (3.3 kΩ) generate an appropriate reference voltage (VREF) of 0.55 V. The 0.02-Ω sense resistor (R17) and VREF of 0.55 V fixes a peak current limit of 2.75 A per 式 2.

2.3.3 Sense Resistor Selection

The selection of sense resistor depends on different factors as follows:

• Required peak current limit from DRV8870 along with VREF pin voltage of DRV8870
• Power dissipation in the sense resistor
• Offset error voltage and gain of the current sense amplifier

The sense resistors are designed to carry a continuous nominal RMS current of 1.5 A and a peak current of 2.75A. A high-sense resistance value increases the power loss in the resistors. A low-sense resistor value increases the error due to input offset voltage of the current sense amplifier at high gain. If the current-sense amplifier is used without offset calibration, select the sense resistor value, so the sense voltage across the resistor is sufficiently higher than the op-amp input offset voltage, which reduces the effect of the offset error. The TLV9061 has a typical input offset error voltage of 0.3 mV (maximum of 1.6 mV). The reference design uses 0.02-Ω sense resistor, and the power loss in sense resistor can be calculated as in 式 3.

Power loss in the resistor $= I_{RMS}^2 \times R_{SENSE} = 1.5^2 \times 0.02 = 0.045$ W

(3)

Using 式 3 at 2.75-A peak current, the power loss in the resistor = 0.151 W (for 1 second)

2.3.4 Current Sense Amplifier

The TLV9061 is used as an external current sense amplifier because of small form factor, good gain bandwidth product (GBW), good slew rate, input EMI filters, rail to rail operation, power supply voltage range, and low offset voltage. This reference design uses the differential amplifier configuration shown in 図 5 with a gain of 24.95 V/V (adjustable with different feedback resistor values). The current is sensed at the DC supply return path, which is normally unidirectional. The current can be bidirectional under regenerative mode support. The bidirectional current sensing is made possible by adding a level shift (V_{REF}) of approximately 1.2 V using the resistors R11 and R12.
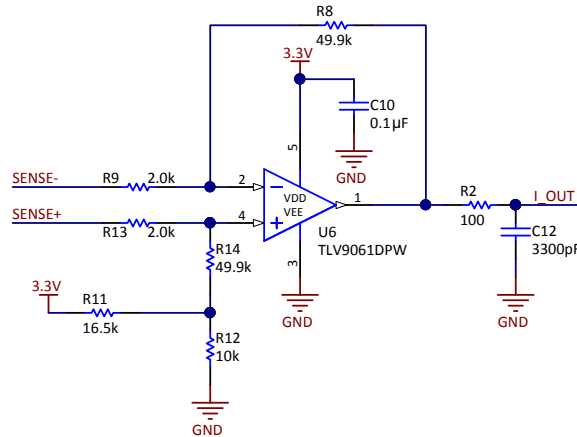
Copyright © 2017, Texas Instruments Incorporated

図 5. TLV9061 Current Sense Amplifier Schematic

注: For accurate voltage level shifting, a reference voltage IC or an op-amp voltage follower circuit can be used to generate the 1.2 V.

The current sense resistor of 20 mΩ, amplifier gain of 24.95, and the level shift of approximately 1.2 V make the amplifier circuit measure the current accurately from –2-A to 3.5-A peak. The output voltage of the amplifier can be approximately calculated using 式 4.

$$V_{OUT} = V_{REF} + (I \times CSA\_GAIN \times R_{ISEN})$$

(4)

The output of the op amp connects to the MCU through the output low-pass filter R2 and C12.

Consider connecting a 0.01-µF ceramic capacitor across the resistor R12 for a noise-free level-shift reference voltage for the op amp and connecting a low-pass filter after the sense resistor and before the amplifier input depending on the layout used.

2.3.5 LDO—3.3-V Generation

The reference design uses the ultra-low quiescent current, LDO linear regulator TPS70933 to generate the 3.3-V power supply for the MCU from the input voltage of 10.8 V. 図 6 shows the schematic of the LDO circuit.
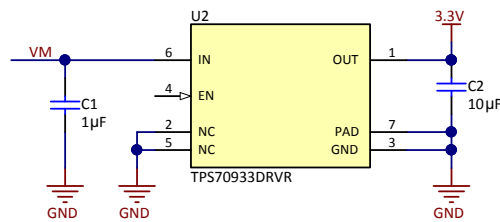
Copyright © 2017, Texas Instruments Incorporated

図 6. Schematic of 3.3-V LDO

The selection of LDO depends on the wide input voltage support (in this design, from 6.5 V to 25.2 V), the load current, and power dissipation. Power dissipation depends on input voltage and load conditions. Power dissipation (P_{diss}) is equal to the product of the output current and the voltage drop across the output pass element, as shown in 式 5.

$$P_{diss} = (V_{IN} - V_{OUT}) \times I_{OUT}$$
(5)

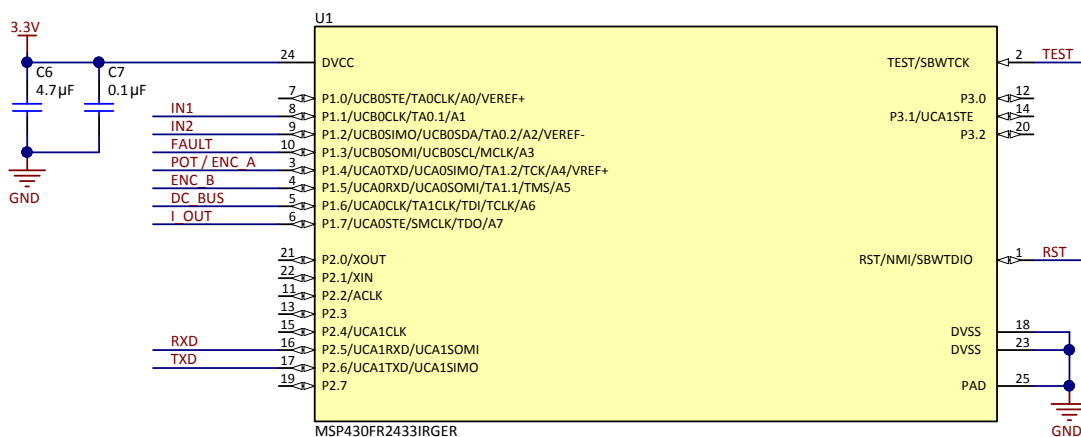Assuming a nominal LDO load current of 20 mA, the power dissipation at V_{IN} = 25.2 V can be calculated as: P_{diss} = (25.2 – 3.3) × 0.02 = 0.438 W. 表 2 shows the specifications of the LDOs used in this reference design. At lower input voltage, the power dissipation in the LDO reduces. This reference design assumes a maximum LDO output current of 30 mA when operating from three-cell Li-ion battery.

表 2. Specification of Buck Converter

PARAMETER	DESIGN SPECIFICATION
Input voltage	6 V to 25.2 V (10.8-V nominal)
Output voltage	3.3 V
Maximum output current	30 mA (at 10.8 V input voltage)

2.3.6   MCU—MSP430FR2433

図 7 shows the configuration of the MSP430FR2433 MCU. The reference design uses 4.7-µF decoupling capacitor (C6). A 0.1-µF capacitor is added to obtain the best performance at a high frequency. The timer A module of the MCU is used for PWM generation. The pin TA0.1 and TA0.2, which generated the necessary PWM output signals, are connected to IN1 and IN2 of the DRV8870. All feedback signals including DC bus voltage, potentiometric analog voltage position feedback, and current sense amplifier output are each mapped to a 10-bit ADC channel of the MCU. The encoder position feedback is connected to the GPIO pins of the MCU, and those GPIO pins are configured for port interrupt on edges. This configuration enables the proper counting of encoder pulses and allows accurate position sensing. The signals TEST and RST are connected to the programming connector. The provision for UART communication is enabled through the pins RXD and TXD.

図 **7. MSP430FR2433 Schematic**

2.3.7   Encoder or Potentiometric Position Feedback

図 8 shows the position feedback interface from the motor to the reference design board. The reference design can support encoder position feedback or a potentiometric analog voltage position feedback. The power supply is 3.3 V for both cases.
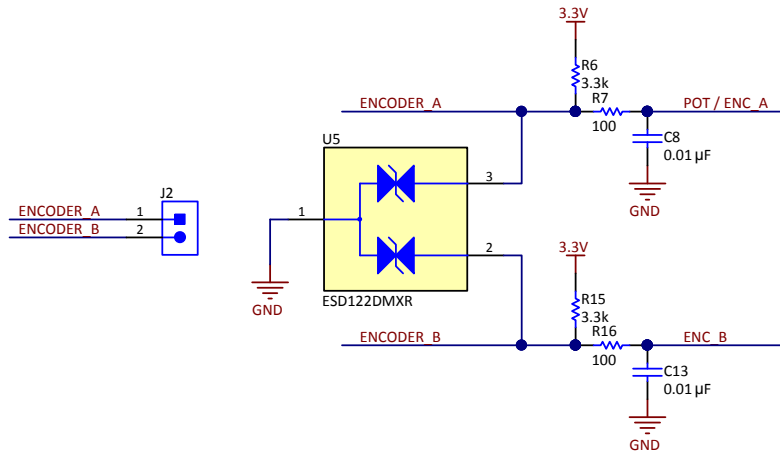

図 8. Motor Position Feedback Schematic

The board can take quadrature encoder output through ENCODER_A and ENCODER_B pin of J2. The interface is protected against ESD using the bidirectional TVS ESD protection diode ESD122. R6 and R15 are used as the pull-up resistors. R7, C8, R16 and C13 forms the low-pass noise filters on each line before feeding to the MCU GPIO pins.

The reference design can also take potentiometric analog voltage position feedback. In that case connect the analog voltage output from the potentiometric position sensor between ENCODER_A and GND. The pull-up resistor R6 may not be required in that case and depends on the position sensor used. If potentiometric feedback is used, configure the P1.4 (connecting the signal POT / ENC_A) port of the MCU as an ADC input.

ブラシ付き*DC*サーボ・ドライブ用、*10.8V/15W*、効率*90%*超、*2.4cm²*電力段のリ
ファレンス・デザイン

3 Hardware, Software, Testing Requirements, and Test Results

3.1 Required Hardware and Software

3.1.1 Hardware

3.1.1.1 Reference Design Board Connector Configuration

図 9 shows the connector configuration of this reference design, which features:

- Two-terminal input for power supply (J3): This pin is used to connect the input DC supply from the battery. The positive and negative terminals can be identified as shown in 図 9.

- Two-terminal output for motor winding connection: The phase output connections for connecting to the BDC motor winding marked as OUT1 and OUT2 as shown in 図 9.

- Three-pin connector J1: This connector is used for external UART communication interface. The RX and TX pins enable the communication with external master controller. The FAULT pin of this connector gives indication on any overcurrent fault in the system.

- Four-pin connector J5: This is the programming connector for the MSP430FR2433 MCU. The two-wire Spy-Bi-Wire protocol is used to program the MSP430FR2433.

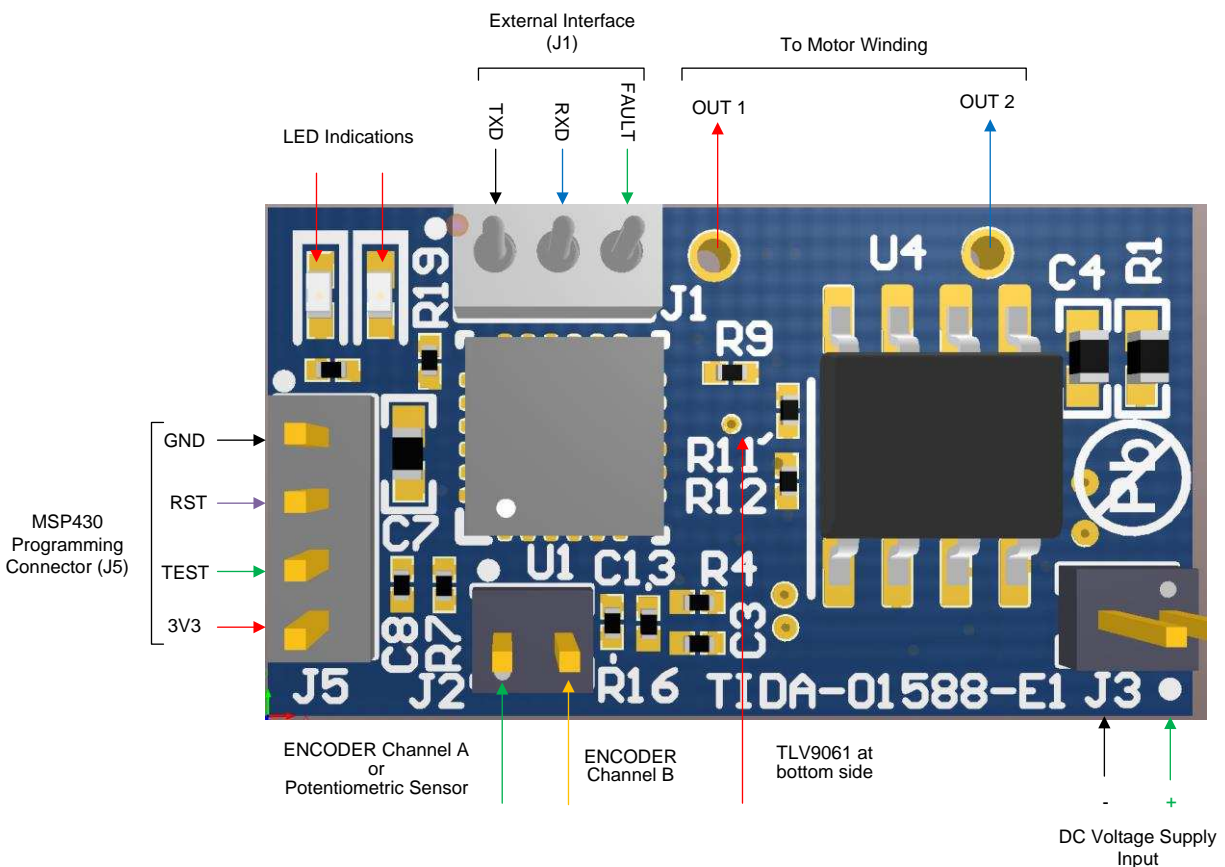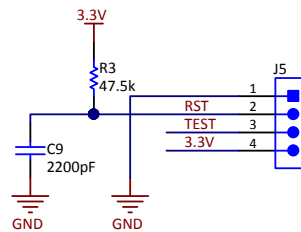- Two-pin connector J2: This connector interfaces the position feedback signals from the motor.

図 9. PCB Connectors

3.1.1.2   Programming the MSP430FR2433

The two-wire Spy-Bi-Wire protocol is used to program the MSP430FR2433 MCU. 図 10 shows the four-pin programming connector provided in the reference design board.

Copyright © 2017, Texas Instruments Incorporated

図 10. Schematic of MSP430FR2433 Programming Connector

See the development tools of the MSP430FR2433 for programming options with an external JTAG interface. Follow these steps to program the MSP430FR2433 MCU when the programming supply voltage is provided by the board itself:

1. Remove the motor connections from the board, and power on the input DC supply. Make sure that a minimum of 8-V DC input is applied and 3.3 V is generated in the board.
2. Connect the programmer to the board.
3. Open the Code Composer Studio™ (CCS) integrated development environment (IDE), and build and debug the code to program the MCU.

3.1.1.3   Procedure for Board Bring-up and Testing

Follow this procedure for board bring-up and testing:

1. Remove the motor connections from the board, and power on the input DC supply. Make sure that a minimum of a 8-V DC input is applied and the 3.3 V is generated in the board.
2. Program the MCU as detailed in 3.1.1.2. Make sure that the configuration in the program is done as per 3.1.2.
3. Remove the programmer, and switch off the DC input supply.
4. Connect the OUT1 and OUT2 outputs to the motor winding terminals.
5. Use a DC power supply with current limit protection and apply 8-V DC to the board. The motor will start rotating and stops at the position mentioned by the position reference.
6. To change direction, switch off the DC input, and correct the IN1 and IN2 logic in the program to reverse the direction of motor rotation and re-load the same in to the MCU.

3.1.2 Software

3.1.2.1 High-Level Description of Application Firmware

The reference design's firmware offers the following features and user controllable parameters:

- Position control using feedback from a two-channel encoder
- Initialization of necessary PWM, ADC, and position feedback capture

表 3 lists the design's firmware system components.

表 3. Firmware System Components

SYSTEM COMPONENT	DESCRIPTION
Development and emulation	Code Composer Studio version 7
Target controller	MSP430FR2433
PWM frequency	20-KHz PWM (default), programmable for higher and lower frequencies
Interrupts	Port 1 Interrupts enabled on P1.4 and P1.5 corresponds to encoder interface.
PWM generation—timer configuration	IN1 – TA0.1; CLOCK = 16 MHz, OUTMOD_6, PWM frequency set for 20 KHz IN2 – TA0.2; CLOCK = 16 MHz, OUTMOD_6, PWM frequency set for 20 KHz
Position feedback—encoder signals	P1.4 → ENCODER_CHANNEL A P1.5 → ENCODER_CHANNEL B
ADC channel assignment	A4 → Potentiometric position feedback A6 → DC bus voltage sensing A7 → DC bus current sensing
MCU digital I/Os	P1.3 → Fault indication (LED2)
UART Communication	P2.5 → RX P2.6 → TX

3.1.2.2 *Customizing the Reference Code*

Select the *main.c* file. Parameters exist at the top of the file that can be optimized and are included as the configuration variables. The following section of code shows these parameters:

#define PWM_PERIOD 400 // PWM Frequency (Hz) = 16MHz / ((2*PWM_PERIOD) - 1)

#define DUTY_CYCLE 70 // Input Duty Cycle inversely relative to PWM_PERIOD

#define REF_ANGLE 90 // Reference angle for Position

#define ENC_RESOLUTION 2.6 //ENC_RESOLUTION (Encoder Resolution) = 360/Encoder pulses in 360 deg rotation

3.1.2.2.1 *PWM_PERIOD*

PWM_PERIOD sets the value in capture and compare register 0 of Timer_A0. The Timer_A0 is initialized to operate at 16 MHz. Use 式 6 to calculate the PWM frequency. The TIMER_A0 PWM is configured in up-down mode.

$$PWM \ Frequency \ (Hz) = \frac{16 \ MHz}{((2 \times PWM\_PERIOD) - 1)}$$

(6)

For example, with PWM_PERIOD = 400, PWM Frequency ≈ 20 kHz

3.1.2.2.2 *DUTY_CYCLE*

Adjust this parameter to control the speed of the motor. This parameter is inversely related to PWM_PERIOD.

3.1.2.2.3 *REF_ANGLE*

REF_ANGLE sets the reference angle of the position reference, which means where to halt the motor.

3.1.2.2.4 *ENC_RESOLUTION*

ENC_RESOLUTION value is calculated as per the number of encoder pulses. The reference design is tested with a motor having a two-channel encoder. Each channel gives 69 pulses in one complete 360° mechanical rotation. The pulses of encoder channel A and channel B are phase shifted. The total number of pulses (by counting both the channels) is 138. Because both of the channels produce phase-shifted pulses to form a quadratic encoder, the effective encoder position resolution (ENC_RESOLUTION) can be calculated using 式 7 as approximately 2.6°.

$$ENC\_RESOLUTION = \frac{360}{Total \ encoder \ pulses \ in \ one \ mechanical \ rotation}$$

(7)

3.1.2.3 *Running the Project in CCS*

To run this project in CCS:

1. Install CCS and import the project *TIDA-01588_Firmware _V1.0*.
2. Read through 3.1.2.2 to customize the code.
3. Power up the board with an external supply as described in 3.1.1.2 and connect the programmer.
4. Build and debug the modified project to download the code to the MSP430FR2433.

3.2 Testing and Results

3.2.1 Test Setup

図 11 shows a representation of the test setup used in the lab to evaluate the TIDA-01588. The reference design is tested with a BDC motor that has the encoder position feedback.
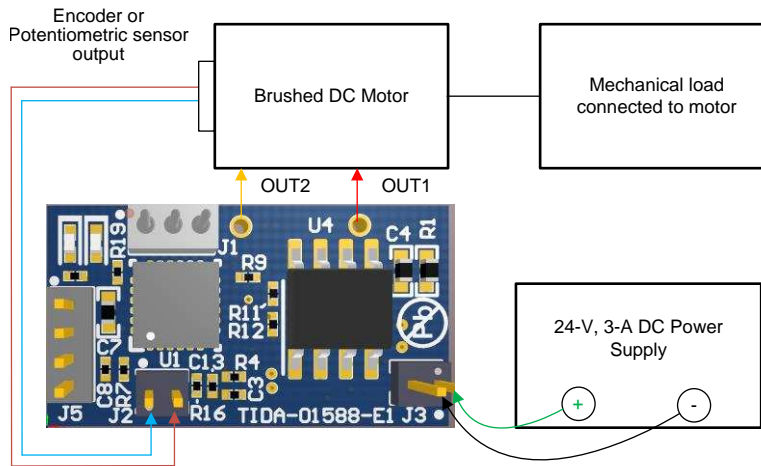

図 11. Test Setup

3.2.2 Power Supply Generated by the LDO—3.3-V

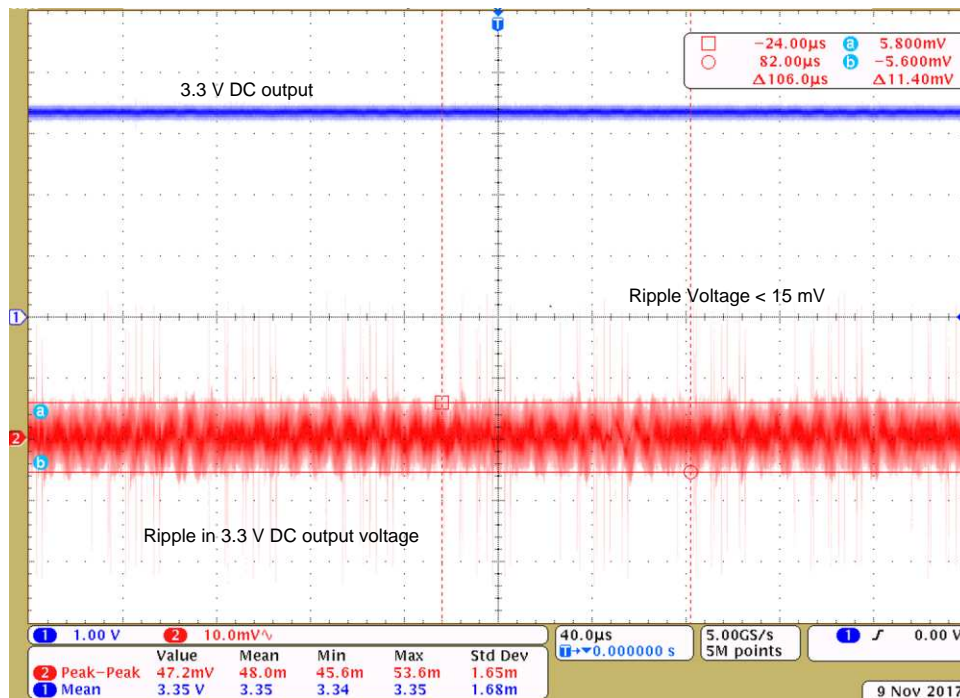図 12 shows the 3.3 V generated from the LDO. The ripple in the 3.3-V rail is less than 15 mV.

図 12. 3.3 V Generated by TPS70933

3.2.3 Testing of Current Sense Amplifier

3.2.3.1 *Current Sense Amplifier Transient Response*

The transient response of the current sense amplifier circuit with TLV9061 is observed by introducing step changes in voltage across the shunt resistor. The step change in sense voltage is created by switching the corresponding half bridge in the DRV8870, which causes the motor current to flow through the sense resistor.

図 13 shows the rising edge transient response of the current sense amplifier for a positive voltage drop across shunt resistor. The motor winding average current is approximately 750 mA. The transient response of the amplifier shows a settling time of approximately 1.5 µs to reach the final steady-state value within 5% dynamic error.
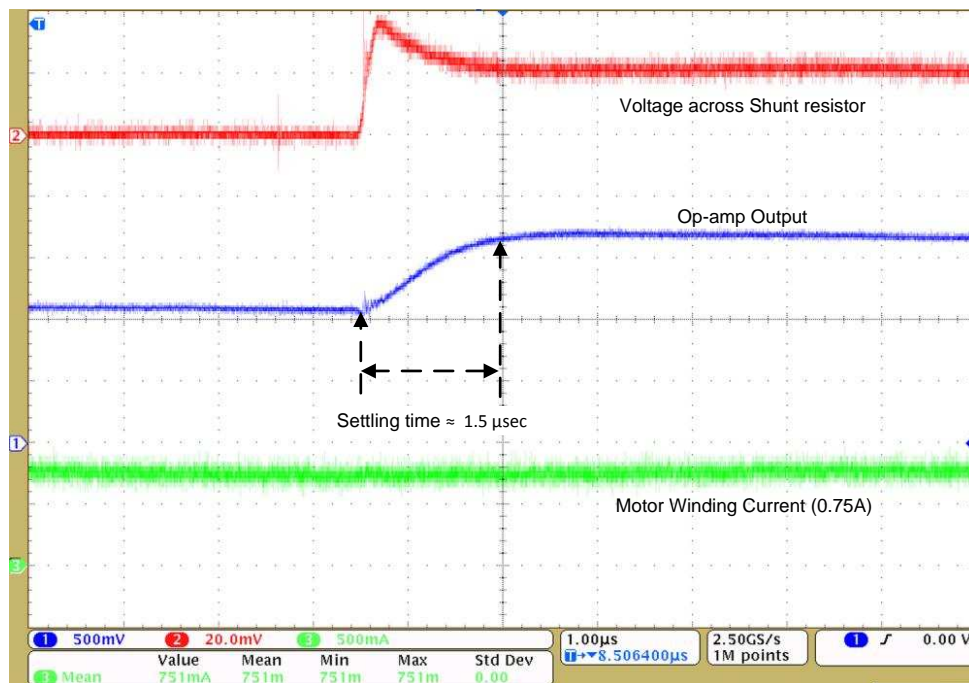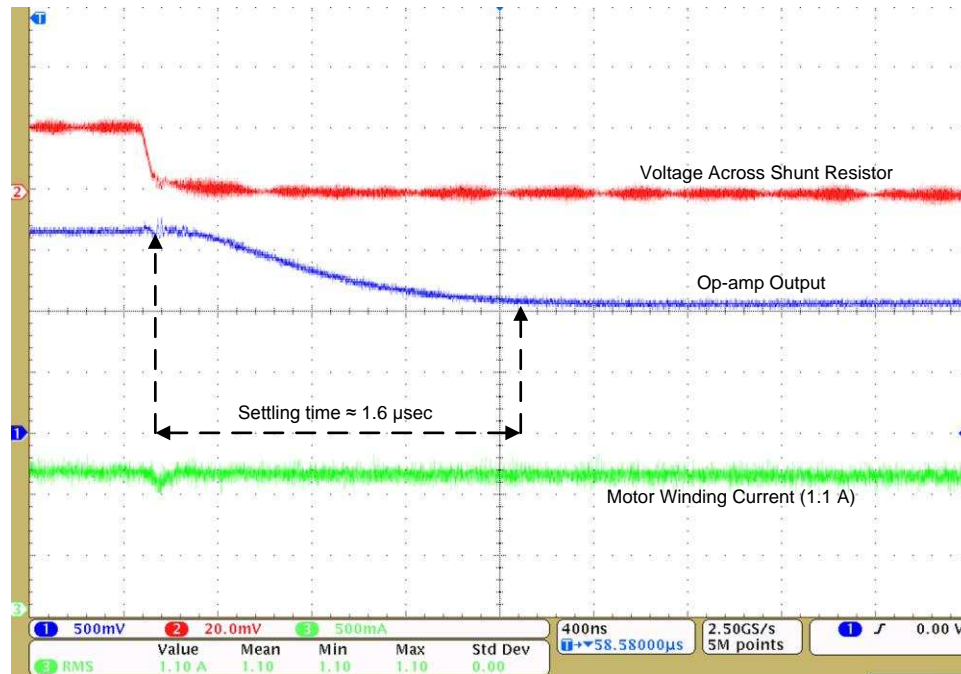

図 13. Rising Edge Step Response of Current Sense Amplifier for Positive Current

図 14 shows the falling edge transient response of the current sense amplifier for a positive voltage drop across shunt resistor. The motor winding average current is approximately 1.1 A. The transient response of the amplifier shows a settling time of approximately 1.6 μs to reach the final steady-state value within 5% dynamic error.

図 **14. Falling Edge Step Response of Current Sense Amplifier for Positive Current**

The high-gain bandwidth (10 MHz) of TLV9061 and the slew rate of 6.5 V/μs enable fast settling and a valid current sample even at low duty cycle. The amplifier has very good stability with good margin, and there is no observable unstable oscillations during transient response. The input EMI filter eliminate any external noise and provides robust performance.

3.2.3.2 *Current Sense Amplifier Transfer Function*

図 15 shows the steady-state transfer function of the DC bus current through the 20-mΩ shunt resistor versus the output voltage of the TLV9061 amplifier. The output voltage equals 1.2 V when the DC bus current is zero. The transfer function is linear, which makes the software processing simple.
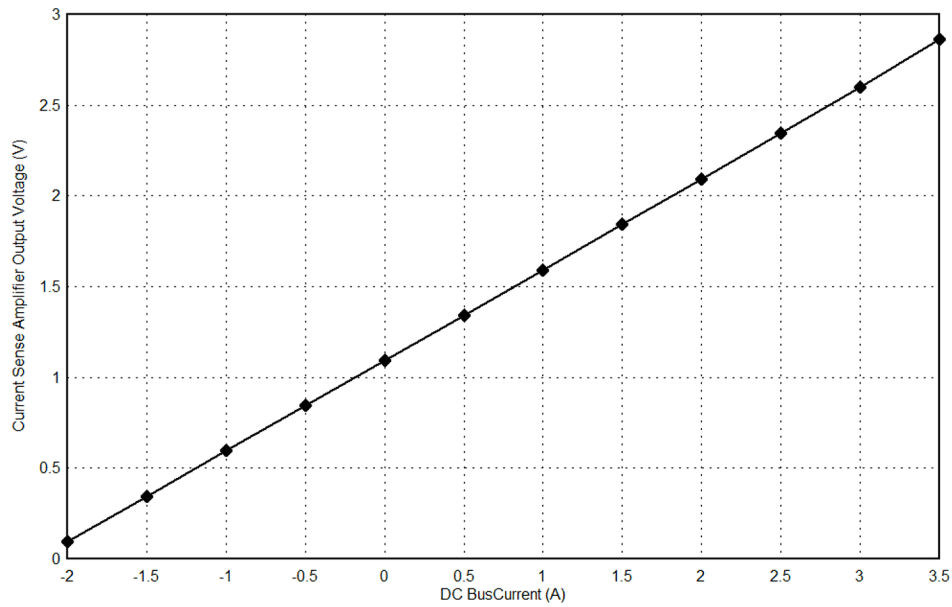

図 15. DC Bus Current-Sensing Transfer Function

3.2.3.3   *DC Bus Current Sensing Accuracy*

This test measures the DC accuracy of the current sense amplifier with a 20-mΩ sense resistor and TLV9061 configured as a single-ended differential amplifier at a gain of 24.95 V/V at 25°C ambient temperature. The full-scale DC bus current measurement range is –2 A to 3.5 A. The DC bus current is measured with a 6½ digit precision multimeter in series to the sense resistor and the output voltage of the current sense amplifier TLV9061 is measured with a 6½ digit precision multimeter. 図 16 shows the absolute error in DC bus current measurement. The uncalibrated absolute error remains within ±0.0.06 A with respect to the input current range from –2 A to 3.5 A. The uncalibrated error is dominated by sense resistor tolerance and offset voltage of opamp.. With op-amp offset voltage calibration, the absolute error reduces to less than ±0.015 A.
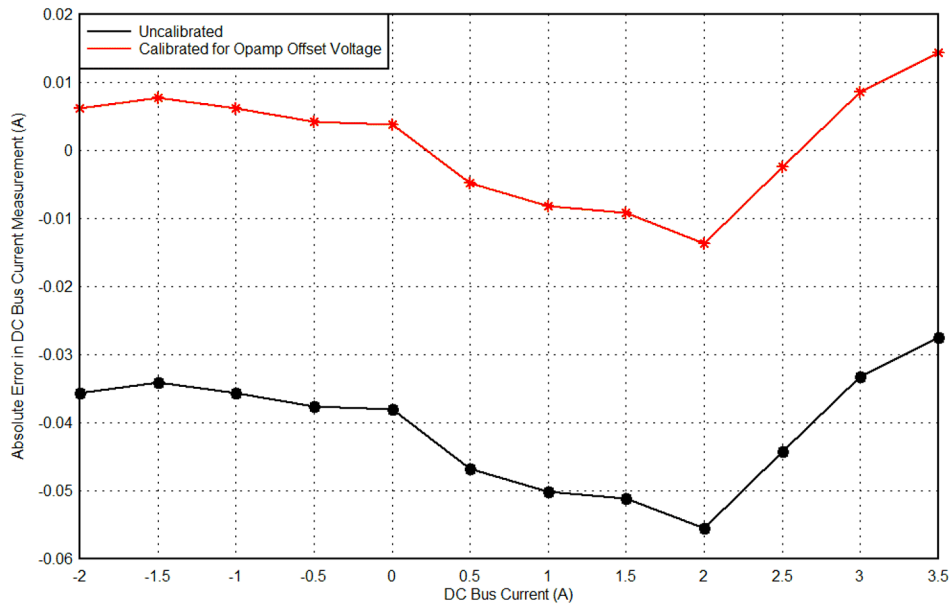

図 16. Absolute Error in DC Bus Current Measurement

図 17 shows the calibrated and uncalibrated relative error [%] in measured current from the op-amp output voltage. The calibrated relative error is less than 1%. The error can be further optimized by using the amplifier gain setting resistors and sense resistor with tight tolerance. The low error enables accurate current sensing and better torque performance from the motor drive.
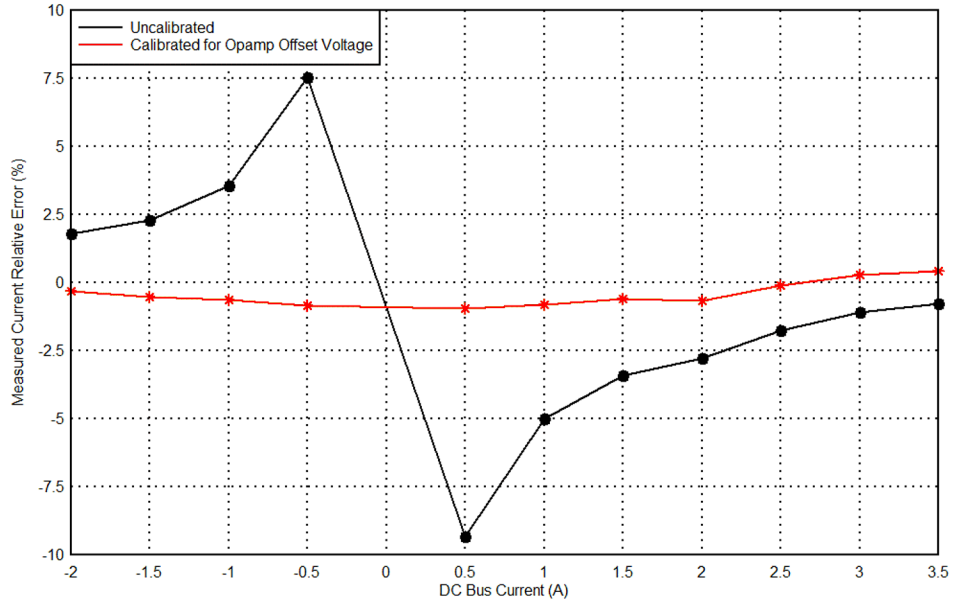

図 17. Relative Error [%] in Measured Current From Amplifier Output Voltage

3.2.4   Functional Testing of DRV8870

The DRV8870 has internal H-bridge power stage consists of four N-channel MOSFETs that are designed to drive current in the motor in both directions. The IN1 and IN2 signals are generated by the MCU, which control the states of DRV8870 drive voltage outputs OUT1 and OUT2 where the DC motor winding is connected. Refer to H-bridge control logic in *DRV8870 3.6-A Brushed DC Motor Driver (PWM Control) Data Sheet*[3].

図 18 shows the functional operation of DRV8870 at the following test conditions:

- IN1—25% PWM at 20-kHz switching frequency
- IN2—100% (High—3.3V)
- Input DC voltage = 10.8 V
- Winding current = 1.5-A RMS

OUT2 switches at approximately 75% pulse width at 20 kHz (when IN1 = 25%) and OUT1 is LOW always, as explained in *DRV8870 3.6-A Brushed DC Motor Driver (PWM Control) Data Sheet*[3].
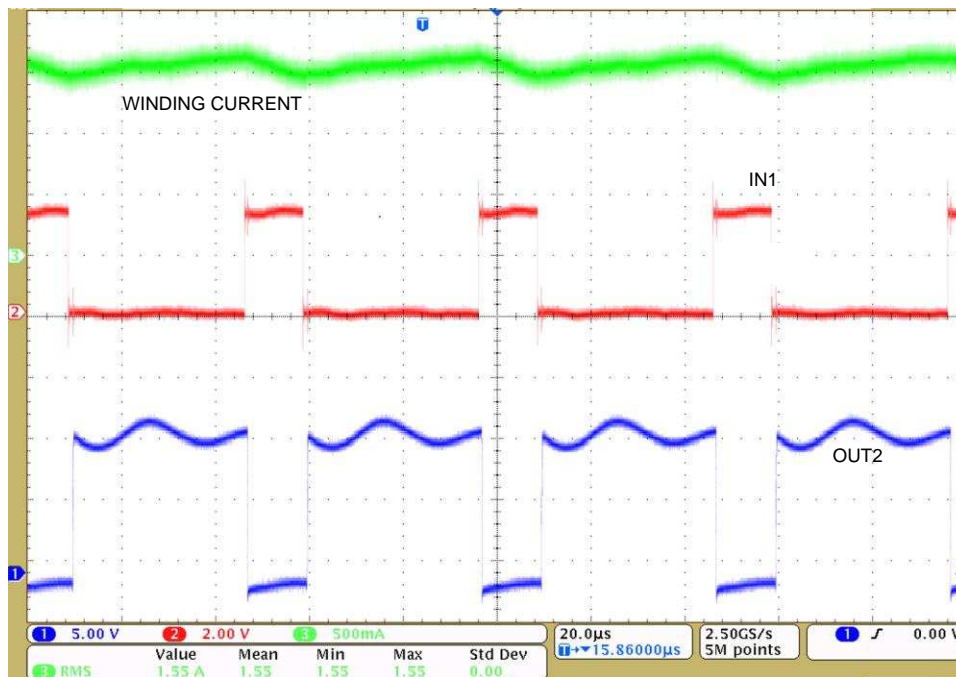

図 18. DRV8870—Functional Evaluation

3.2.5 Load Test

The load test is performed with a BDC motor at 10.8-V DC, and the motor is loaded to 1.4-A RMS. 図 19 shows motor winding current and the output voltage with 95% duty cycle. The maximum temperature observed on DRV8870 is 98°C after 10 minutes of continuous running. No airflow is used during testing. Considering 98°C temperature of DRV8870 being high at 25°C ambient temperature, a small chip size heat sink can be attached to take the current of 1.4 A to enable the operation even at 55°C ambient temperature.

表 4. Load Test Results at 10.8-V DC, 95% Duty Cycle

INPUT DC VOLTAGE (V)	INPUT DC CURRENT (A)	WINDING CURRENT (RMS) (A)	INPUT POWER (W)	MAXIMUM TEMPERATURE ON DRV8870(°C)
10.8	1.52	1.4	16.4	98
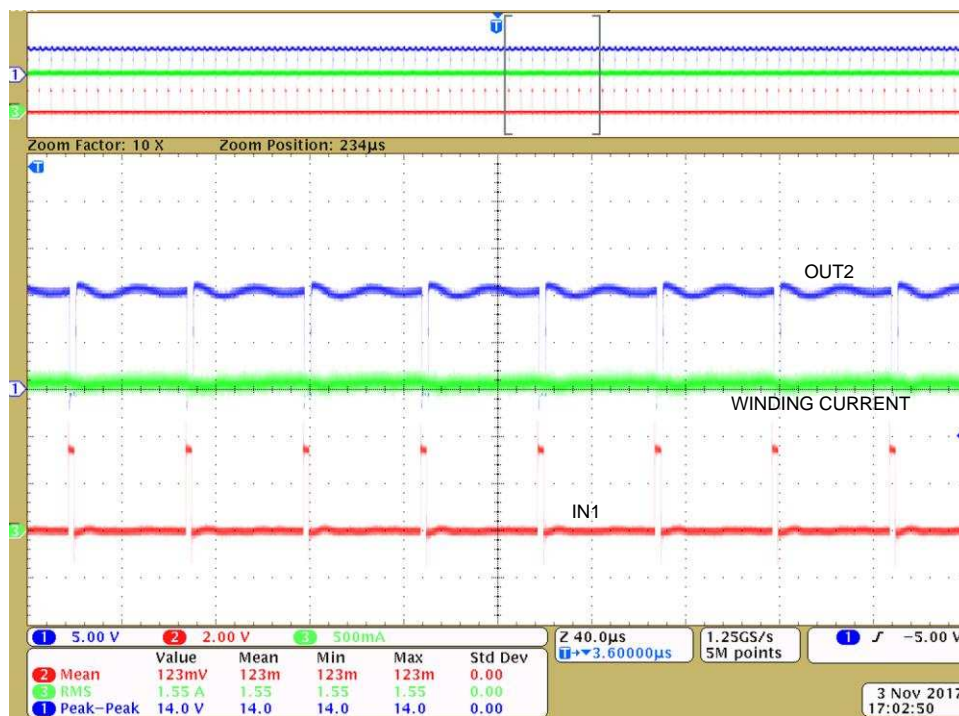
図 19. Load Test Results at 10.8-V DC Input, 1.4-A RMS Winding Current, 95% Duty Cycle
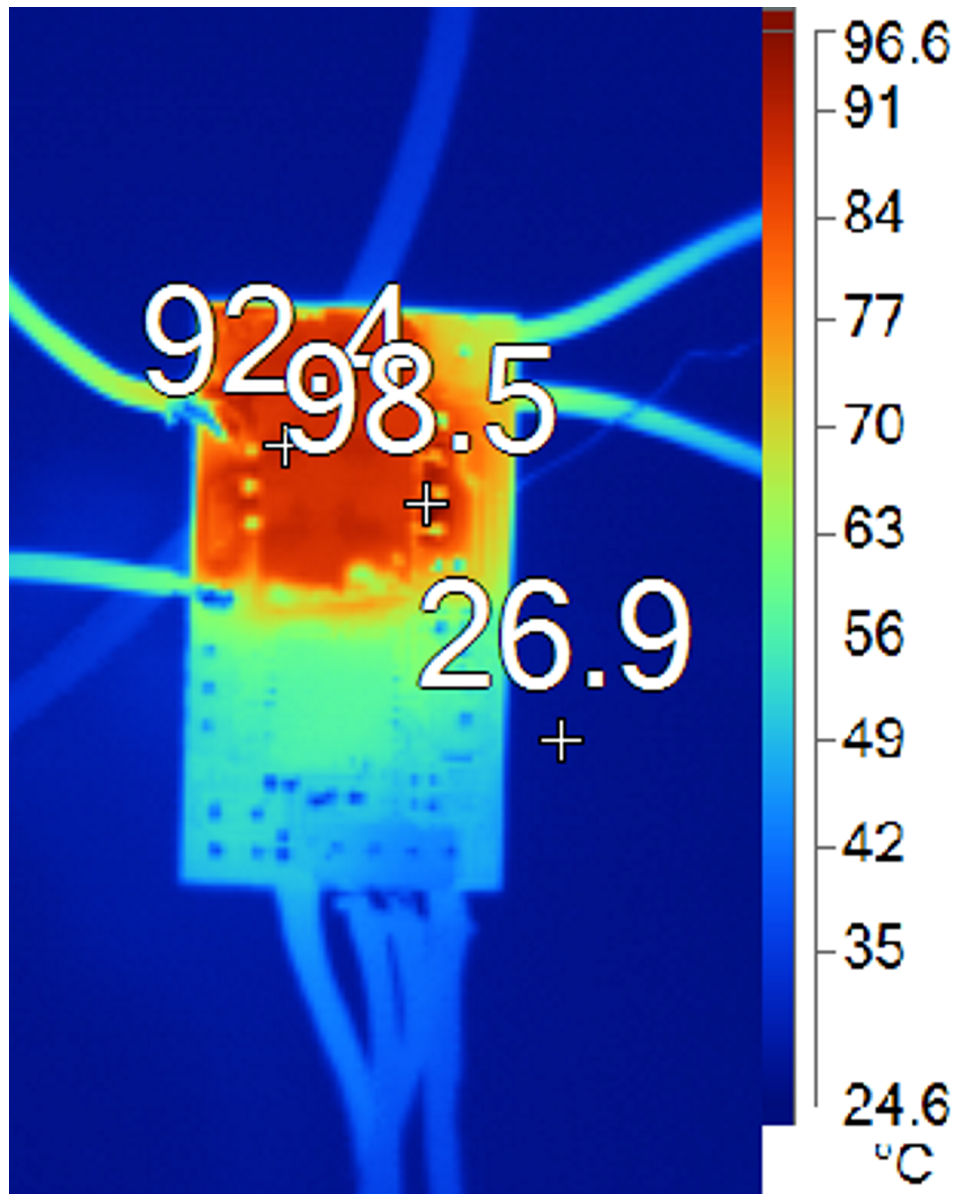
図 20. Thermal Image at 10.8-V DC Input, 1.4-A RMS Winding Current, 95% Duty Cycle

3.2.6 Load Test at Minimum and Maximum Voltages

The reference design can support a minimum DC input voltage of 6.5 V and a maximum input voltage of 25.2 V . 図 21 shows the test load test results at 6.5-V DC bus voltage and 1.5-A RMS motor current at 95% duty cycle. 図 22 shows the test load test results at 25.2-V DC bus voltage and 1.5-A RMS motor current at 95% duty cycle.

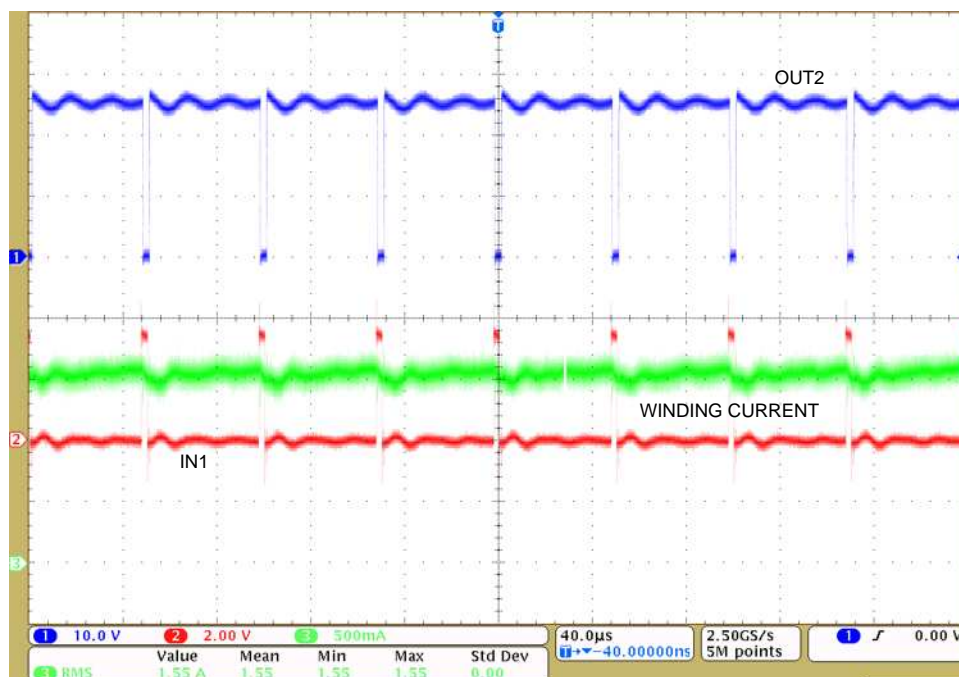図 21. Load Test Results at 6.5-V DC Input, 1.5-A RMS Winding Current, 95% Duty Cycle

図 22. Load Test Results at 25.2-V DC Input, 1.5-A RMS Winding Current, 95% Duty Cycle

3.2.7 Power Stage Efficiency Test

The reference design board power stage efficiency is experimentally tested with a BDC motor load. 表 5 lists the test results without heat sink at a 100% duty cycle. 表 6 lists the test results without heat sink at a 95% duty cycle.

表 5. Inverter Efficiency Test Results at 100% Duty Cycle Without Heat Sink and Without Airflow

INPUT DC VOLTAGE (V)	INPUT DC CURRENT (A)	INPUT DC POWER (W)	MOTOR WINDING RMS CURRENT(A)	BOARD OUTPUT POWER (W)	EFFICIENCY (%)
10.79	0.1134	1.220	0.1083	1.161	95.14
10.76	0.2190	2.355	0.2138	2.270	96.41
10.85	0.3194	3.465	0.3172	3.348	96.62
10.79	0.4807	5.187	0.4800	4.986	96.12
10.80	0.6250	6.747	0.6201	6.446	95.54
10.83	0.7536	8.157	0.7490	7.732	94.79
10.80	0.8683	9.376	0.8635	8.820	94.07
10.86	1.0427	11.318	1.0380	10.496	92.74
10.80	1.2666	13.683	1.2612	12.484	91.24
10.87	1.4156	15.384	1.4104	13.912	90.43

表 6. . Inverter Efficiency Test Results at 95% Duty Cycle Without Heat Sink and Without Airflow

INPUT DC VOLTAGE (V)	INPUT DC CURRENT (A)	INPUT DC POWER (W)	MOTOR WINDING RMS CURRENT(A)	BOARD OUTPUT POWER (W)	EFFICIENCY (%)
10.84	0.1138	1.233	0.1145	1.169	94.78
10.79	0.1975	2.132	0.2027	2.040	95.67
10.78	0.3216	3.467	0.3338	3.332	96.10
10.82	0.4830	5.226	0.5039	4.984	95.38
10.87	0.5983	6.501	0.6266	6.165	94.83
10.82	0.7200	7.788	0.7548	7.320	93.99
10.79	0.8382	9.041	0.8797	8.408	93.00
10.82	1.0081	10.910	1.0596	10.011	91.76
10.78	1.2594	13.580	1.3247	12.296	90.54
10.75	1.4293	15.368	1.5050	13.801	89.80

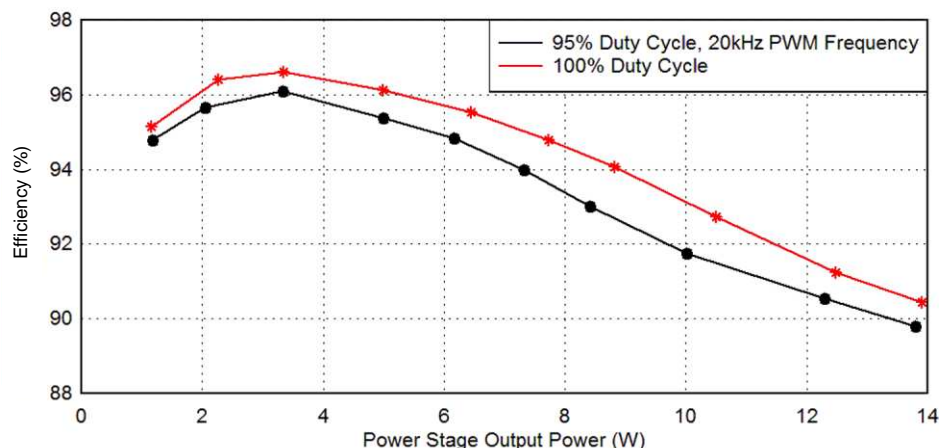The efficiency curve of these test conditions are plotted in 図 23.

図 23. Power Stage Efficiency Versus Output Power

The low $R_{DS(ON)}$ of the motor driver DRV8870 ensure low power loss in the device and enable efficiency more than 90%. The exposed thermal pad of DRV8870 along with enough PCB copper area having multiple vias ensure efficient heat dissipation to the PCB. Refer to *DRV8870 3.6-A Brushed DC Motor Driver (PWM Control) Data Sheet*[3] to understand the power loss calculation and heat dissipation while designing with DRV8870.

3.2.8   Overcurrent Limit Results

The overcurrent limit is set by the voltage at the VREF pin of DRV8870 and the sense resistor value, which is explained in 2.3.2. For a fixed sense resistor value, the overcurrent limit can be set by adjusting the VREF voltage, which is done by modifying the resistor values of R10 and R5.

When overcurrent trip level (ITRIP) is reached, the device enforces slow current decay by enabling both low-side FETs. The device enforces slow current decay for a time of t_{OFF} (typically 25 μs). After t_{OFF} elapses, the output is re-enabled according to the two inputs, INx. The drive time (t_{DRIVE}) until reaching another ITRIP event heavily depends on the VM voltage, the back-EMF of the motor, and the inductance of the motor.

図 24 shows the overcurrent trip operation with a VREF = 0.35 V, using 20-mΩ sense resistor. Using the 式 2, the expected overcurrent trip is 1.75 A, and the observed overcurrent trip is approximately 1.6 A.
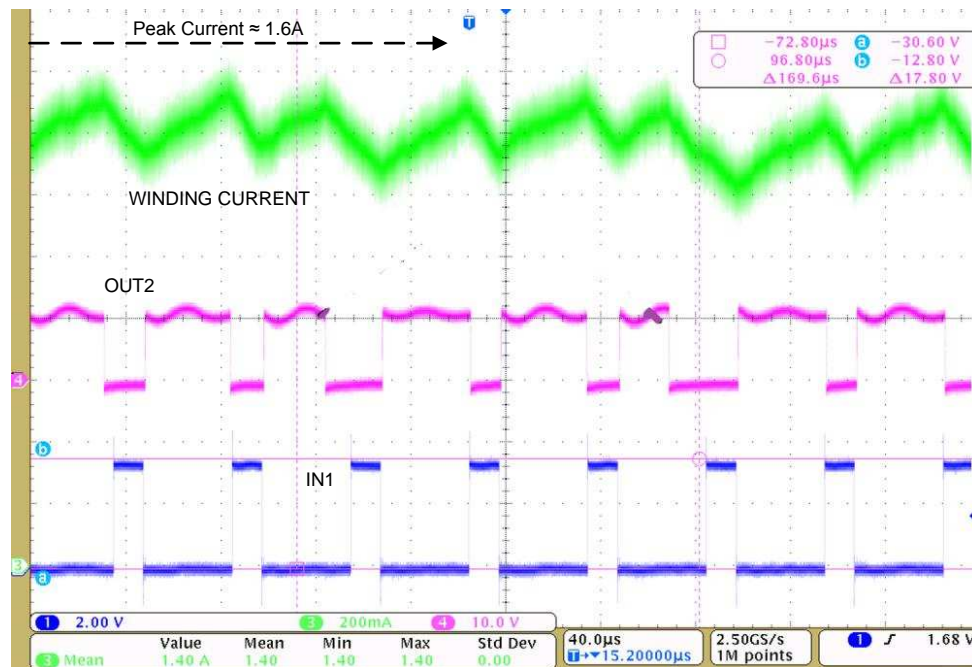

図 24. Overcurrent Trip at VREF = 0.35 V With 20-mΩ Sense Resistor

図 25 shows the overcurrent trip operation with a VREF = 0.55 V (R10 = 16.5 k, R5 = 3.3 k), using 20-mΩ sense resistor. The observed overcurrent trip is approximately 2.5 A.
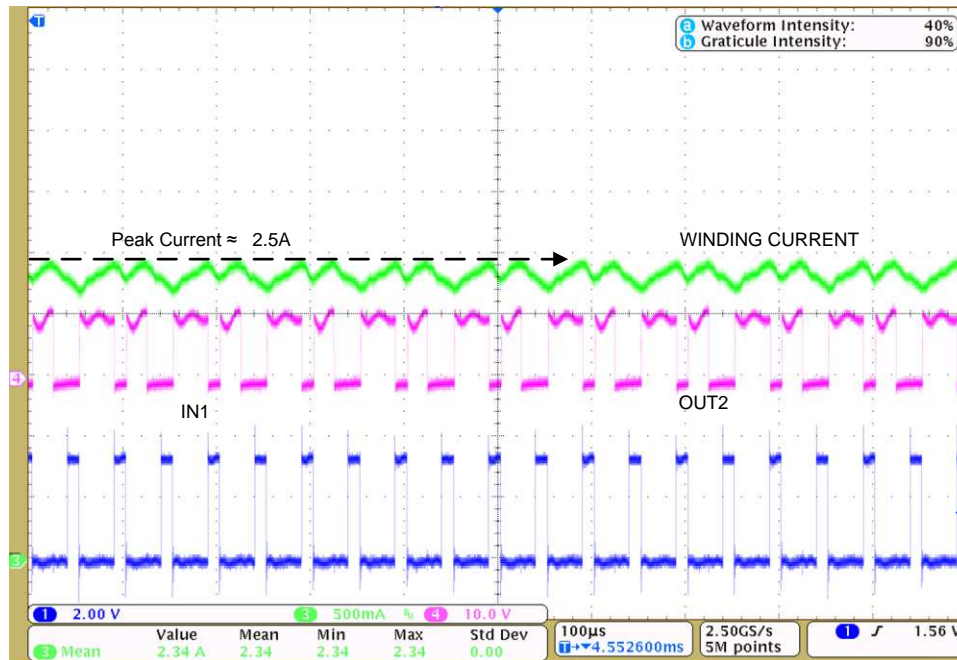

図 25. Overcurrent Trip at VREF = 0.55 V With 20-mΩ Sense Resistor

注: The error between the set current limit and observed current limit is less than 10%. The tolerance of the sense resistor, accuracy of set VREF voltage and tolerance in DRV8870 ISEN gain are the major contributors of current limit error. The error can be reduced by calibrating above mentioned factors.

3.2.9   Peak Current Test Results

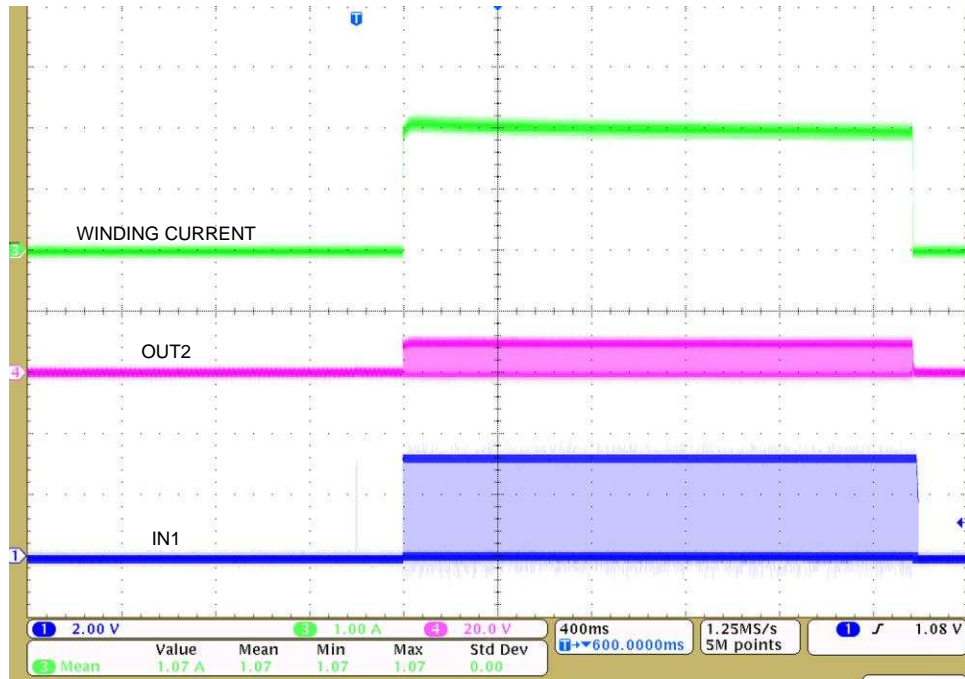図 26 shows the winding current of 2-A when the motor is stalled for more than 2 s.

図 26. Peak Current of 2-A in Motor Winding

図 27 shows the thermal image of the board after 2 s. The maximum temperature observed on the DRV8870 is 89.7°C.
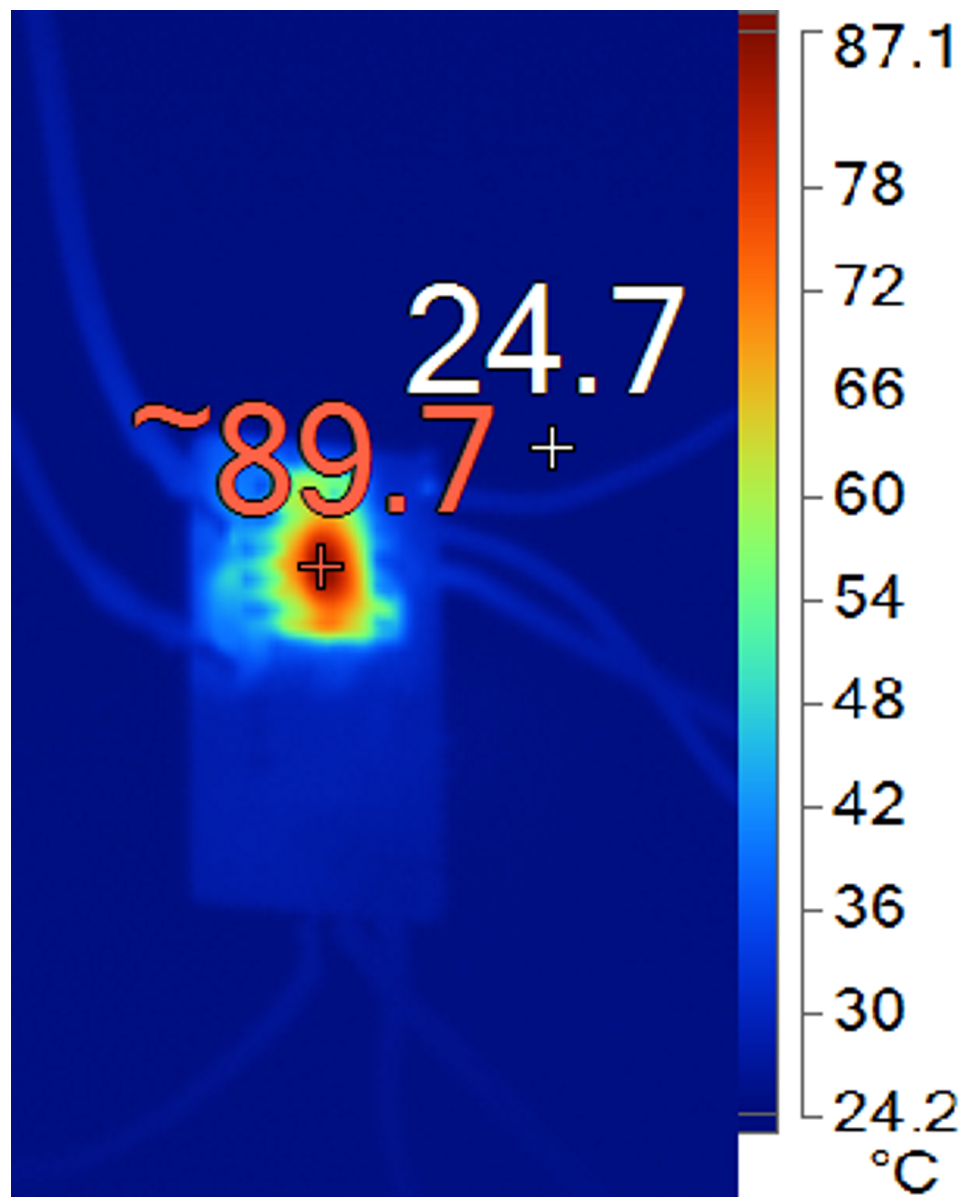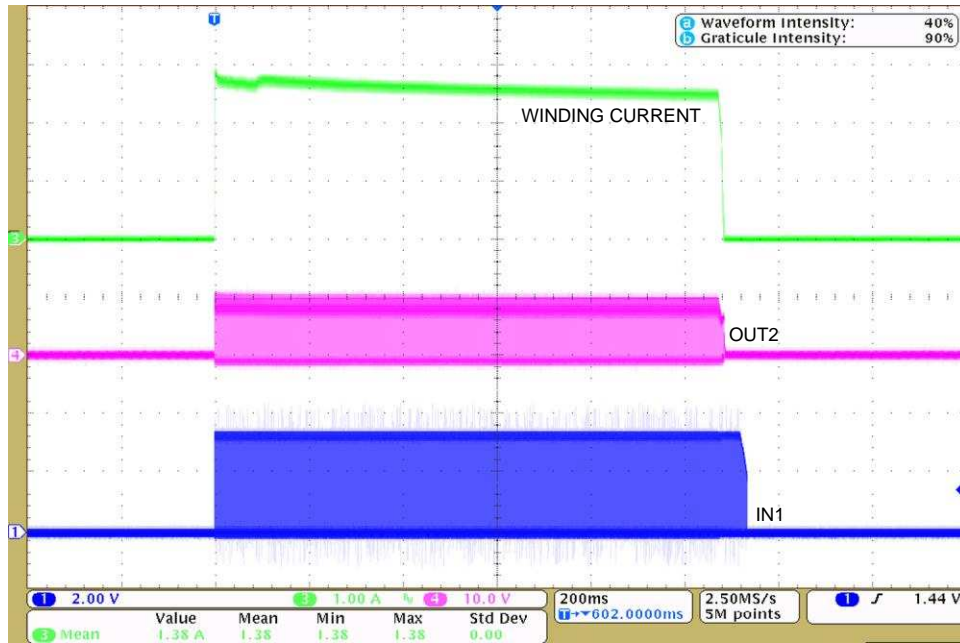

図 **27. Thermal Image of Board After 2 s With 2-A Peak Current in Motor Winding**

図 28 shows the winding current of 2.7 A when the motor is stalled for 1 s.

図 28. Peak Current of 2.7 A in Motor Winding

図 29 shows the thermal image of the board after 1 s. The maximum temperature observed on the DRV8870 is 92.1°C.
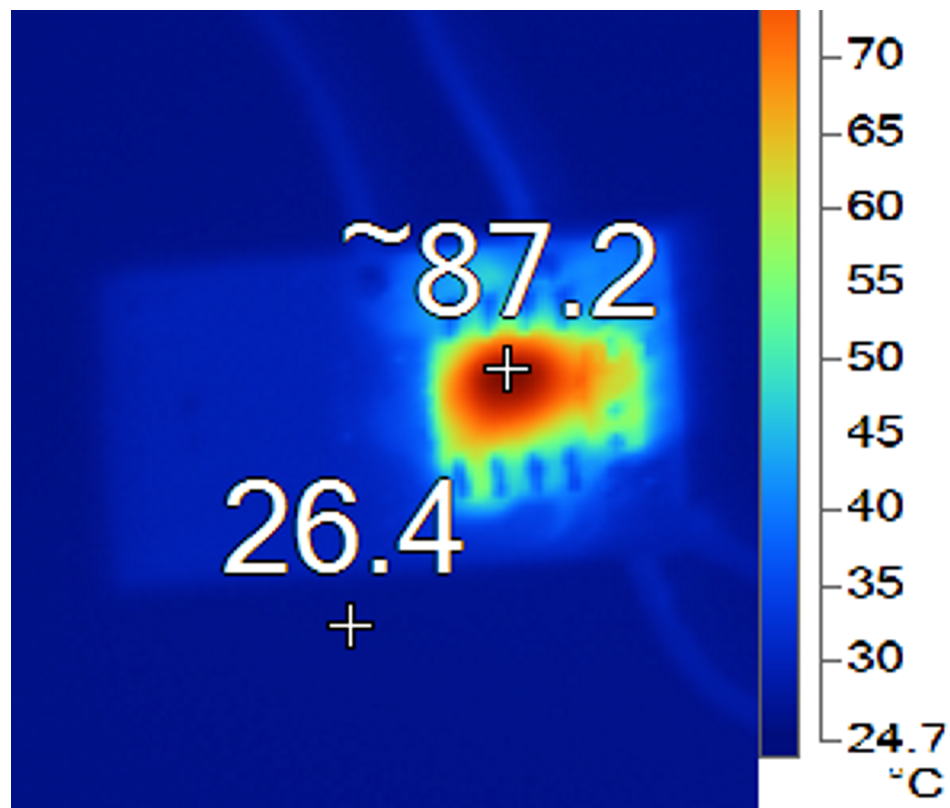

図 29. Thermal Image of Board After 1 s With 2.7-A Peak Current in Motor Winding

3.2.10 BDC Motor Position Control With TIDA-01588

The position control algorithm on MSP430FR2433 is implemented using port interrupts capability of the MCU. The testing is done on BDC motor which has inbuilt quadrature encoder. Each channel of quadrature encoder gives 69 pulses in one complete mechanical rotation of the motor. The resolution of the encoder interface can be calculated in 式 7.

With this motor, the motor position can be measured up to 2.6° accurate and MCU is programmed accordingly. The testing was done to hold the motor position at 90° mechanical (¼ rotation) and 180° mechanical (half rotation) .
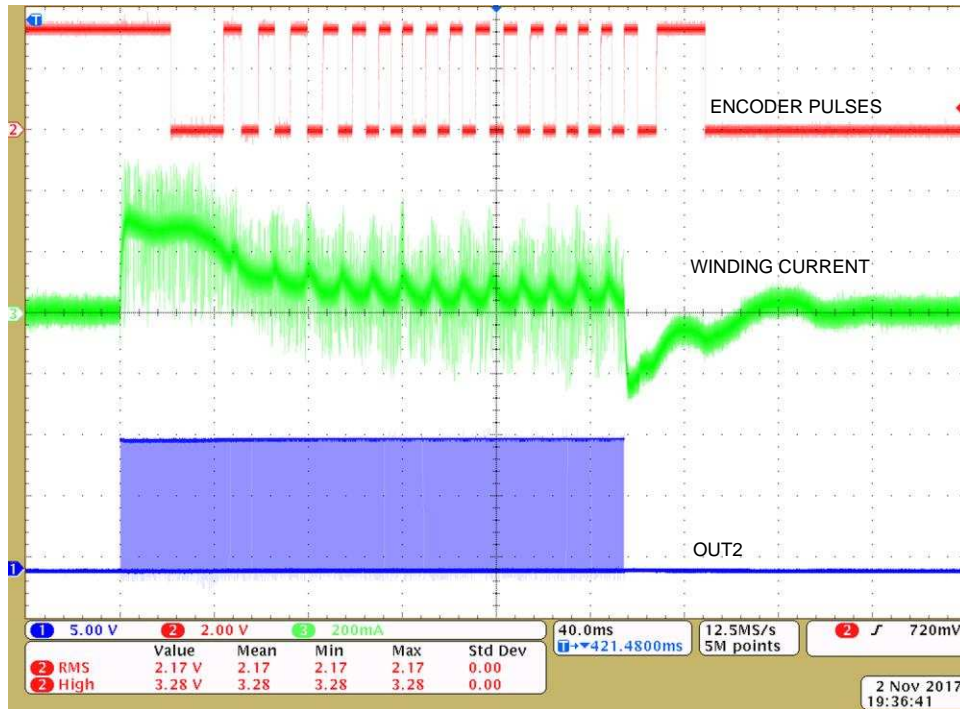

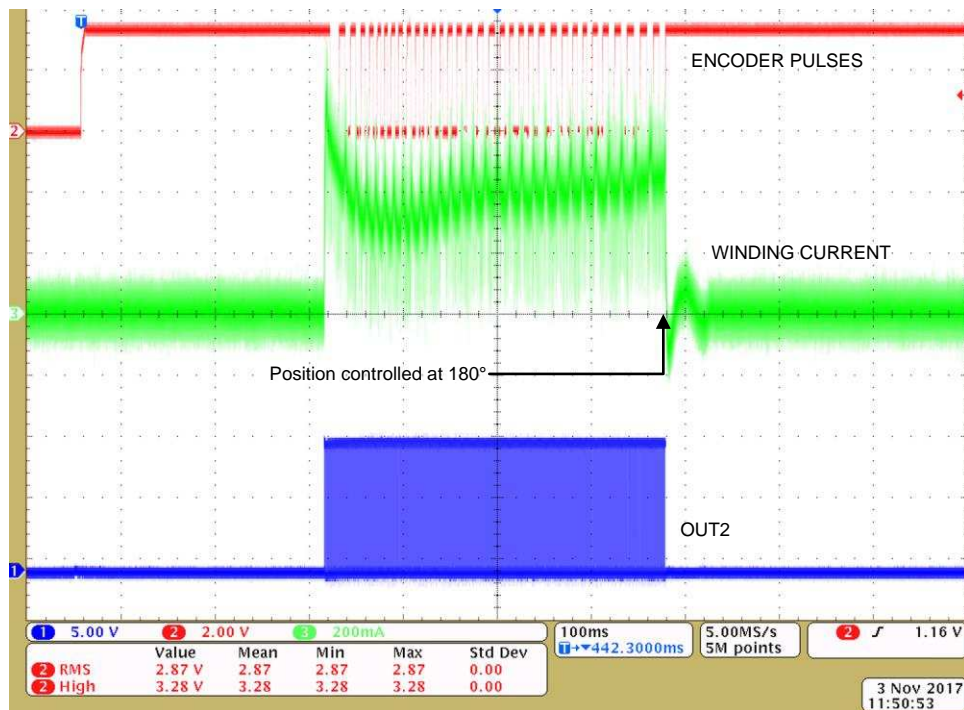図 30. Test Results for Position Control of Motor After One-Fourth Rotation

図 31. Test Results for Position Control of Motor After Half Rotation

4   Design Files

4.1   Schematics

To download the schematics, see the design files at TIDA-01588.

4.2   Bill of Materials

To download the bill of materials (BOM), see the design files at TIDA-01588.

4.3   PCB Layout Recommendations

The bulk capacitor for DRV8870 must be placed to minimize the distance of the high-current path through the motor driver device. The connecting metal trace widths must be as wide as possible, and numerous vias must be used when connecting PCB layers. These practices minimize inductance and allow the bulk capacitor to deliver high current. Small-value capacitors must be ceramic and placed closely to device pins. The high-current device outputs must use wide metal traces. The DRV8870 thermal pad must be soldered to the PCB top-layer ground plane. Multiple vias must be used to connect to a large bottom-layer ground plane. The use of large metal planes and multiple vias help dissipate the I² x $R_{DS(ON)}$ heat that is generated in the device.

4.3.1   Layout Prints

To download the layer plots, see the design files at TIDA-01588.

4.4   Altium Project

To download the Altium project files, see the design files at TIDA-01588.

4.5   Gerber Files

To download the Gerber files, see the design files at TIDA-01588.

4.6   Assembly Drawings

To download the assembly drawings, see the design files at TIDA-01588.

5   Software Files

To download the software files, see the design files at TIDA-01588.

6   Related Documentation

1. Texas Instruments, *PowerPAD™ Thermally Enhanced Package Application Report*
2. Texas Instruments, *Current Recirculation and Decay Modes Application Report*
3. Texas Instruments, *DRV8870 3.6-A Brushed DC Motor Driver (PWM Control) Data Sheet*

6.1   商標

E2E, PowerPAD, MSP430, Code Composer Studio are trademarks of Texas Instruments.
すべての商標および登録商標はそれぞれの所有者に帰属します。

7   Terminology

BDC—Brushed DC motor

ESD—Electrostatic discharge

MCU—Microcontroller unit

PWM— Pulse width modulation

8 About the Author

VARAD JOSHI is a project trainee in the Industrial Systems team at Texas Instruments, where he is learning and developing reference design solutions with a focus on Motor drive systems. Varad is a final-year student pursuing a bachelor of engineering (B.E. hons) in electrical and electronics engineering from Birla Institute of Technology & Sciences (BITS), Pilani, Goa.

MANU BALAKRISHNAN is a systems engineer at Texas Instruments, where he is responsible for developing subsystem design solutions for the Industrial Motor Drive systems. Manu brings to this role his experience in power electronics and analog and mixed signal designs. He has system level product design experience in permanent magnet motor drives. Manu earned his bachelor of technology in electrical and electronics engineering from the University of Kerala and his master of technology in power electronics from National Institute of Technology Calicut, India.

JASRAJ DALVI is an End Equipment Lead with Industrial Systems team at Texas Instruments, where he is responsible for defining reference design solutions and control algorithms for motor control systems. He completed his Bachelors of Engineering degree in Electrical Engineering from University of Pune, India and his Post Graduate Diploma in Marketing Management at S.I.B.M. in Pune, India.

TIの設計情報およびリソースに関する重要な注意事項

Texas Instruments Incorporated ("TI")の技術、アプリケーションその他設計に関する助言、サービスまたは情報は、TI製品を組み込んだアプリケーションを開発する設計者に役立つことを目的として提供するものです。これにはリファレンス設計や、評価モジュールに関係する資料が含まれますが、これらに限られません。以下、これらを総称して「TIリソース」と呼びます。いかなる方法であっても、TIリソースのいずれかをダウンロード、アクセス、または使用した場合、お客様(個人、または会社を代表している場合にはお客様の会社)は、これらのリソースをここに記載された目的にのみ使用し、この注意事項の条項に従うことに合意したものとします。

TIによるTIリソースの提供は、TI製品に対する該当の発行済み保証事項または免責事項を拡張またはいかなる形でも変更するものではなく、これらのTIリソースを提供することによって、TIにはいかなる追加義務も責任も発生しないものとします。TIは、自社のTIリソースに訂正、拡張、改良、およびその他の変更を加える権利を留保します。

お客様は、自らのアプリケーションの設計において、ご自身が独自に分析、評価、判断を行う責任がお客様にあり、お客様のアプリケーション(および、お客様のアプリケーションに使用されるすべてのTI製品)の安全性、および該当するすべての規制、法、その他適用される要件への遵守を保証するすべての責任をお客様のみが負うことを理解し、合意するものとします。お客様は、自身のアプリケーションに関して、(1) 故障による危険な結果を予測し、(2) 障害とその結果を監視し、および、(3) 損害を引き起こす障害の可能性を減らし、適切な対策を行う目的での、安全策を開発し実装するために必要な、すべての技術を保持していることを表明するものとします。お客様は、TI製品を含むアプリケーションを使用または配布する前に、それらのアプリケーション、およびアプリケーションに使用されているTI製品の機能性を完全にテストすることに合意するものとします。TIは、特定のTIリソース用に発行されたドキュメントで明示的に記載されているもの以外のテストを実行していません。

お客様は、個別のTIリソースにつき、当該TIリソースに記載されているTI製品を含むアプリケーションの開発に関連する目的でのみ、使用、コピー、変更することが許可されています。明示的または黙示的を問わず、禁反言の法理その他どのような理由でも、他のTIの知的所有権に対するその他のライセンスは付与されません。また、TIまたは他のいかなる第三者のテクノロジまたは知的所有権についても、いかなるライセンスも付与されるものではありません。付与されないものには、TI製品またはサービスが使用される組み合わせ、機械、プロセスに関連する特許権、著作権、回路配置利用権、その他の知的所有権が含まれますが、これらに限られません。第三者の製品やサービスに関する、またはそれらを参照する情報は、そのような製品またはサービスを利用するライセンスを構成するものではなく、それらに対する保証または推奨を意味するものでもありません。TIリソースを使用するため、第三者の特許または他の知的所有権に基づく第三者からのライセンス、あるいはTIの特許または他の知的所有権に基づくTIからのライセンスが必要な場合があります。

TIのリソースは、それに含まれるあらゆる欠陥も含めて、「現状のまま」提供されます。TIは、TIリソースまたはその仕様に関して、明示的か暗黙的かにかかわらず、他のいかなる保証または表明も行いません。これには、正確性または完全性、権原、続発性の障害に関する保証、および商品性、特定目的への適合性、第三者の知的所有権の非侵害に対する黙示の保証が含まれますが、これらに限られません。

TIは、いかなる苦情に対しても、お客様への弁護または補償を行う義務はなく、行わないものとします。これには、任意の製品の組み合わせに関連する、またはそれらに基づく侵害の請求も含まれますが、これらに限られず、またその事実についてTIリソースまたは他の場所に記載されているか否かを問わないものとします。いかなる場合も、TIリソースまたはその使用に関連して、またはそれらにより発生した、実際的、直接的、特別、付随的、間接的、懲罰的、偶発的、または、結果的な損害について、そのような損害の可能性についてTIが知らされていたかどうかにかかわらず、TIは責任を負わないものとします。

お客様は、この注意事項の条件および条項に従わなかったために発生した、いかなる損害、コスト、損失、責任からも、TIおよびその代表者を完全に免責するものとします。

この注意事項はTIリソースに適用されます。特定の種類の資料、TI製品、およびサービスの使用および購入については、追加条項が適用されます。これには、半導体製品(http://www.ti.com/sc/docs/stdterms.htm)、評価モジュール、およびサンプル(http://www.ti.com/sc/docs/sampterms.htm)についてのTIの標準条項が含まれますが、これらに限られません。